

# Light versus Dark in Strong Lensing Galaxies: Dark matter halos are rounder than their stars

Claudio Bruderer<sup>1\*</sup>, J. I. Read<sup>1,2</sup>, P. Saha<sup>3</sup>, J. Coles<sup>4</sup>

<sup>1</sup>*Institute for Astronomy, Department of Physics, ETH Zürich, Wolfgang-Pauli-Strasse 27, CH-8093 Zürich, Switzerland*

<sup>2</sup>*Department of Physics, University of Surrey, Guildford, GU2 7XH, UK*

<sup>3</sup>*Institute for Theoretical Physics, University of Zürich, Winterthurerstrasse 190, 8057 Zürich, Switzerland*

<sup>4</sup>*Department of Biology and Health, Versailles Saint-Quentin-en-Yvelines University, France*

2 December 2014

## ABSTRACT

We measure the shape and alignment of stars and dark matter in 11 strong lensing galaxies with good quality data. We find that in all cases the dark matter halos are more elliptical than the light distribution over the range  $R_e < R < 5R_e$ . As we average over larger radii, the lenses become increasingly elliptical both in their dark matter and stars, but dark matter halos are never more elliptical than  $s_{dm} = 1.15$ , while their stars can extend to  $s_* > 1.4$  (where  $s$  is the ratio of the largest to smallest eigenvalue of the 2D moment of inertia tensor). Three systems have very high stellar ellipticity ( $s_* > 1.6$ ) and correspondingly high alignment between light and dark. One of these – B1608 – is a known merging pair; we suggest that the other two (B0712 and B2016) may also be recent post-merger systems. Galaxies with high dark matter ellipticity and weak external shear show very strong alignment between light and dark; those with strong shear ( $\gamma \gtrsim 0.1$ ) can be very highly misaligned. This is reassuring since isolated misaligned galaxies are expected to be unstable.

Our results provide a new constraint on galaxy formation models that must explain the origin of very round dark matter halos (not expected in pure dark matter only simulations), and highly misaligned systems. Such misalignments also present a new challenge for alternative gravity theories in which the light and dark must necessarily be highly correlated.

**Key words:** Gravitational lensing: strong — galaxies: structure

## 1 INTRODUCTION

The ellipticity and shape of stars relative to their host dark matter halo encodes information both about our cosmological model ( $\Lambda$ CDM) and galaxy formation (e.g. Dubinski 1994; Ibata et al. 2001; Kazantzidis et al. 2004; Macciò et al. 2007; Debattista et al. 2008; Lux et al. 2012; Read 2014). ‘Dark-matter-only’ (DMO) simulations in  $\Lambda$ CDM predict dark matter halos that are triaxial (Dubinski & Carlberg 1991; Warren et al. 1992; Navarro et al. 1996; Jing & Suto 2002), with mean ‘shape parameter’  $\langle q \rangle = (b + c)/2a \sim 0.8$  (where  $a > b > c$  are the long, intermediate and short axes of the figure; Macciò et al. 2007). This corresponds to a typically *prolate* halo. However, including ‘baryons’ (stars and gas) in the models produces halos that are significantly rounder and – at least for disc galaxies – well-aligned with the light distribution (Katz & Gunn 1991; Dubinski 1994; Debattista et al. 2008). Halo shapes and alignments also con-

strain alternative gravity models (Mortlock & Turner 2001; Helmi 2004; Read & Moore 2005; Ferreras et al. 2012; Debattista et al. 2013). If the visible light is the only source of gravity in a galaxy, then we expect the light and mass distribution to be highly correlated; if dark matter is present, however, such correlations can, at least in principle, be broken.

Strong lensing provides a unique probe of the alignment and shape of the total mass distribution in galaxies (e.g. Blandford & Narayan 1986; Schneider et al. 1992; Keeton et al. 1998; Kochanek et al. 2000; Koopmans et al. 2006; Auger et al. 2007; Ferreras et al. 2008; Auger et al. 2010; Leier et al. 2012). For ‘red and dead’ ellipticals that are largely devoid of gas, their baryonic content can be mapped through stellar population synthesis modelling of their light distribution (e.g. Ferreras et al. 2005; Treu et al. 2006; Ferreras et al. 2008). This opens up the possibility of directly comparing the light and mass in strong lensing systems (Keeton et al. 1998; Ferreras et al. 2008; Treu et al. 2009; Sluse et al. 2012). Previous work in the literature has found

\* E-mail: claudio.bruderer@phys.ethz.ch

that the light and mass are well-aligned (though a mis-match of up to  $10^\circ$  is not uncommon; e.g. Sluse et al. 2012). However, results on the ellipticity of light and mass agree less well, with Sluse et al. (2012) finding a strong correlation and Keeton et al. (1998) and Ferreras et al. (2008) finding none. It is difficult, however, to compare the results between these different studies because they use different lens modelling techniques; different definitions of ellipticity; and different radii over which the shapes and alignments are probed. Furthermore, none to date have applied their methodology to mock data to determine the robustness of the results.

Weak lensing can also be used to probe the shape and alignment between light and dark, but only for ‘stacked’ galaxies (Brainerd & Wright 2000; Natarajan & Refregier 2000). Hoekstra et al. (2004) applied this idea to data from the Red-Sequence Cluster Survey (RCS) to measure the first weak lensing signal of halo flattening. They found that dark matter halos appear to be rounder than their light distributions, with some weak evidence for alignment. Both measurements are challenging, however, and more recent data appear to be at odds with this early work, favouring dark matter halos that are more elliptical than their stars (Mandelbaum et al. 2006; Parker et al. 2007; van Uitert et al. 2012).

Recently, we introduced a new non-parametric lens tool, GLASS (Coles et al. 2014). Applying this to a large suite of mock data, we showed that mass and light can only reliably be disentangled in strong lensing systems if: i) there are at least four images; and ii) time delay data are available and/or the stellar mass dominates the potential over the region of the images. In this paper, we collate data of the above quality, compiling a sample of 11 strong lens galaxies. We apply GLASS to these lenses to non-parametrically measure the shape and alignment of the stars and *dark matter* in these lensing galaxies, for the first time. This differs from previous works that have all compared the light distribution with the total mass, rather than the dark matter. Since the stars often dominate the central potential, the total mass naturally correlates with the light, potentially masking theoretically interesting results about the dark matter distribution. Our comparison between light and dark is made possible by the fact that GLASS uses the light distribution as a prior on the mass map, ensuring that the dark matter mass is always positive.

This paper is organised as follows. In §2, we briefly review the GLASS code. In §3, we present our data compilation with references. In §4, we present our results. Finally, in §5 we discuss the implications of these results and we present our main conclusions.

## 2 GLASS: A NON-PARAMETRIC LENS TOOL

GLASS (Gravitational Lensing Analysis Software) is a new ‘non-parametric’ lens modelling framework. (Non-parametric here simply means that we deliberately use many more parameters than data constraints such that our system of equations is under-constrained.) GLASS shares some aspects with an earlier code PIXELEN (??). However, GLASS – which contains all new code written from the ground up – significantly improves upon PIXELEN in several key ways:

- (i) At the heart of GLASS is a new uniform sampling algo-

rithm for high dimensional spaces (?). This allows for large ensembles of  $> 10,000$  models to be efficiently generated.

- (ii) GLASS provides a modular framework that allows new priors to be added and modified easily.

- (iii) The basis functions approximating a model can be easily changed (in this paper, we assume pixels as in PIXELEN).

- (iv) With so many models in the final ensemble, we can afford to apply non-linear constraints (for example stellar kinematic data; or the removal of models with spurious extra images) to accept/reject models in a post-processing step.

- (v) The central region of the mass map can have a higher resolution to more efficiently capture steep models.

- (vi) Stellar density can be used as an additional constraint on the models.

- (vii) Point or extended mass objects can be placed in the field.

GLASS is described in detail in the code paper: Coles et al. (2014). Here, we simply list the default priors we use to model each lens. Where the priors differ from these defaults for any given lens, this is spelled out in data Table 2:

- (i) Observational priors (redshifts, image positions relative to lens position).

- (ii) Image parity is enforced.

- (iii) Reconstructed stellar mass map.

- (iv) Local density gradient is always pointing within  $50^\circ$  to the center and the slope is at most 0 everywhere. In other words, the density profile peaks in the center.

- (v) Fixed cosmology:  $\Omega_m = 0.28$ ,  $\Omega_\Lambda = 0.72$ ,  $\Omega_k = 0$ ,  $H_0^{-1} = 13.7$  Gyr.

- (vi) A flat prior on the magnitude of the external shear  $|\gamma|$  on  $[0, 1]$ .

In case of more information, the following priors can be turned on:

- (vii) A flat prior on measured time delays within the  $\pm 1\sigma$ -interval.

- (viii) External point masses to model satellite galaxies outside but close to the Einstein radius.

- (ix) Point symmetry  $\kappa(x, y) = \kappa(-x, -y)$  in case there is reason to assume the surface mass profile to be symmetric (3+1 quad configurations and the double *Q0957*).

### 2.1 Measuring the shape and alignment of a lens

**JR. WE NEED TO DEFINE OUR SHAPE PARAMETER AND ANALYSIS METHOD HERE. JR. WE NEED TO ALSO DEFINE  $R_e$  HERE AND EXPLAIN THAT WE AVERAGE SHAPE OVER  $1-5R_e$**

## 3 DATA

**JR. CLAUDIO TO ADD DATA HERE.**

**Content:**

- Describe data set (why this data set, special features of galaxies (environment: y/n/unknown, elliptical/disk))

- **JR. Claudio to add this bit?**

*Q0047-2808* (hereafter *Q0047* or *0047*) is a luminous early-type galaxy (?). ? find a group of 9 members all of which they spectroscopically confirm.

*MG0414+0534* (hereafter *0414*) is a passively evolving early-type galaxy (?). ? find a very close luminous satellite galaxy north-west of the lens. Due to the proximity of this satellite, we include it as a point mass in our analysis.

*B0712+472* (hereafter *0712*) is an early-type galaxy (?). Another galaxy, 102" to the south-east seems to be at a similar redshift (?). There is also a group of 10 galaxies at a lower redshift.

*RXJ0911+0551* (hereafter *0911*) is an almost circular early-type galaxy (Sluse et al. 2012). It has measured time delays (?). It lies on the outskirts of a cluster (?). This cluster seems to be rather complex and especially it is not spherical. Possibly it is not dynamically relaxed, although X-ray emission can be detected. Analysis of this emission yields a temperature of 2.3 keV. There is also a satellite galaxy to the north-west direction (?).

*Q0957+561* (hereafter *0957*) is a cD galaxy lying close to the center of a cluster with a high spiral galaxy-fraction (e.g. ???). Due to the large image separation, large physical scales are probed. As listed in Table 3 of ?, the position angles to the center of the cluster of earlier lens reconstructions range between 51.8 deg and 67.8 deg measured north-through-east. These results are consistent with the center of the X-ray emission from the cluster (?). The lens has a measured time delay, e.g. (?). They however also find a three-day lag between the g- and r-bands, and the estimates do not agree at the  $2\sigma$ -level. They argue that this effect can be accounted for by the presence of a substructure and chromatic dispersion. We find that the results do not change significantly for either estimate and choose therefore the g-band measurement.

*PG1115+080* (hereafter *1115*) is an early-type galaxy (?). It has measured time delays. We use recent estimates of the time delays by ? which differ significantly from traditional values by e.g. ?. ? and ? analyzed the environment of the lens thoroughly. It is part of a small group of 13 members. ? detect also X-ray emission from the corresponding group, which yields a temperature of 0.8 keV.

*B1422+231* (hereafter *1422*) is an early-type galaxy (?). Although there are measured time delays by ?, they are probably not to be trusted too much as they deviate significantly from theoretical expectations in ?. An accurate measurement of the time delays would require time delay measurements on the scale of hours. ? find a group environment with 16 spectroscopically confirmed member galaxies. Using newer data, ? find an additional member. ? also detect X-ray emission from the corresponding group at a temperature of 1.0 keV.

*B1608+656* (hereafter *1608* or *1608*) consists of two merging galaxies. The main galaxy is an early-type galaxy which is disrupted by a smaller, probably late-type galaxy (?). The system has measured time delays (?). The environment and the mass distribution along the line of sight have been analyzed by ?. They find a group with 8 resp. 9 members if the merging galaxies are counted as 2. No significant X-ray emission was detected from the surrounding group (?). Along the line of sight seem to be four other groups.

*MG2016+112* (hereafter *2016*) is a giant elliptical galaxy (?). It is the farthest lens we consider in this sam-

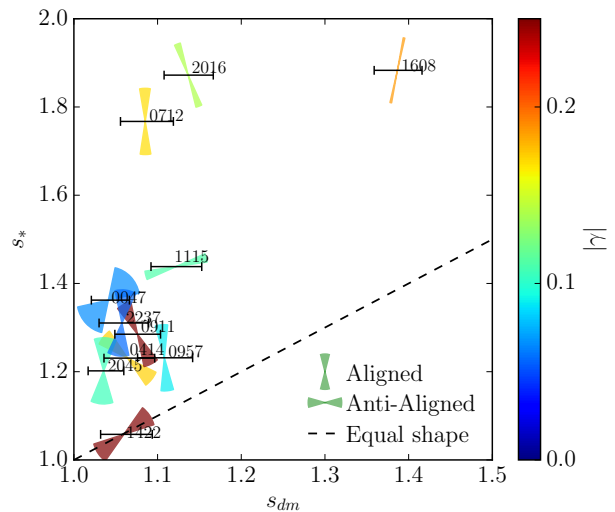


Figure 1.

ple. It lies in a cluster which consists of 69 probable galaxies (?). The clusters shows a high density of galaxies close to the lens in a south-east direction.

*B2045+265* (hereafter *2045*) is probably an elliptical galaxy (?). ? initially classified the galaxy as a late-type Sa galaxy, the velocity dispersion however seems too high. As the source redshift is rather low, a large lens mass is needed. ? therefore conclude that it is more likely an elliptical galaxy. To the west of the lens, ? find that a group at a similar redshift as the lens. ? also find evidence for a dwarf satellite galaxy. As the measurements are not conclusive, we chose to treat the lens as an isolated object.

*Q2237+030* (hereafter *2237*) is a barred spiral (?). With only a redshift of  $z = 0.04$ , it is the closest lens of the sample. Due to the low redshift, the probed physical scales are quite small. No further inquiries into the environment were made.

Further information about the sample can be found in ?, ?, and Sluse et al. (2012).

## 4 RESULTS

### JR. CLAUDIO OR JUSTIN TO WRITE RESULTS SECTION? Content:

- Describe special features in reconstructed lenses
- Show the wedges money plot
- Discuss the results, especially:
  - 1. Dark matter halos seem quite round, stars not necessarily
  - 2. Both DM and stars more elliptical with increasing radius
  - 3. DM halos with weak shear are aligned (apart from spherical systems that don't count); strong shear systems can be highly misaligned.
  - 4. No sensitivity to shear prior. Only one lens B2045 requires a shear prior to avoid spurious extra images; doesn't affect the shape measure though.
  - 5. Merger systems stand out.

Lens	$z_L$	$z_S$	$\Delta\theta$ [kpc]	$R_L/R_e$	Environment
0047	0.485	3.60	12.82	$1.45 \pm 0.04$	G(9)
0414	0.960	2.64	16.01	$1.85 \pm 0.05$	...
0712	0.410	1.34	6.82	$1.15 \pm 0.03$	...
0911	0.769	2.8	23.16	$3.09 \pm 0.05$	C
0957	0.356	1.41	29.98	$3.51 \pm 0.04$	C
1115	0.310	1.72	10.76	$2.94 \pm 0.06$	G(13)
1422	0.337	3.62	6.02	$4.49 \pm 0.06$	G(17)
1608	0.630	1.39	13.92	$1.82 \pm 0.01$	!CHECK!
2016	1.010	3.3	26.22	$6.12 \pm 0.14$	C(69)
2045	0.870	1.28	14.46	$1.48 \pm 0.03$	!SEE TEXT!
2237	0.039	1.7	1.40	$0.89 \pm 0.01$	...

**Table 1.** Table with lens properties (see ?). References in Section 3 expand

Lens	A ["]	B ["]	C ["]	D ["]	Time delays [days]	Additional priors
0047	1.270	-0.630	0.520	-0.730	...	None
	0.105	-0.995	-1.045	0.705		
0414	-0.472	-1.061	-1.1947	0.885	...	None
	1.277	-0.661	-0.255	-0.361		
0712	-0.013	0.795	0.747	-0.391	...	None
	-0.804	-0.156	-0.292	0.307		
0712	-0.013	0.795	0.747	-0.391	...	None
	-0.804	-0.156	-0.292	0.307		
0957 <sup>a</sup>	1.408	0.182	2.860	-1.540	$\Delta t_{BA} = 416.5^{+1}_{-1}$	Symm
	5.034	-1.018	3.470	-0.050		
1115	0.355	-0.909	-1.093	0.717	$\Delta t_{BA} = 12.0^{+2}_{-2}$ $\Delta t_{DC} = 4.4^{+3.2}_{-2.4}$	None
	1.322	-0.714	-0.260	-0.627		
1422	1.079	0.357	0.742	-0.205	...	Symm
	-0.095	0.973	0.656	-0.147		
1608	-1.300	-0.560	-1.310	0.570	$\Delta t_{BA} = 31.5^{+2}_{-1}$ $\Delta t_{CA} = 36.0^{+1.5}_{-1.5}$ $\Delta t_{DA} = 77.0^{+2}_{-1}$	None
	-0.800	1.160	0.700	-0.080		
2016	-1.735	0.335	0.437	1.268	...	None
	1.778	-1.450	-1.435	0.276		
2045	1.121	1.409	1.255	-0.507	...	$\gamma(0.1)$ , Symm
	0.824	0.035	0.576	-0.183		
2237	0.598	-0.075	0.791	-0.710	...	None
	0.758	-0.939	-0.411	0.271		

**Table 2.** Table with lens properties relevant for modelling (positions, time delays)<sup>a</sup> Images A and B are a pair, C and D the other expand

## 5 CONCLUSION

We have measured the shape and alignment of stars and dark matter in 11 strong lensing galaxies using a new non-parametric lens tool, GLASS. We focussed on lenses that have either time delay data or stellar mass maps that contribute significantly to the central potential, since these have data quality good enough to determine the projected shape of their dark matter halos (Coles et al. 2014). We measured the shape and alignment using the eigenvalues  $\lambda$  and vectors of the 2D moment of inertia tensor of the stars and dark matter, defining a *shape parameter*  $s = \lambda_{\max}/\lambda_{\min}$  (§2.1). We averaged  $s$  over the range  $1-5R_e$ , where  $R_e$  is the effective radius of the light profile.

Our key results are as follows:

- We found that in all cases the dark matter halos are more elliptical than the light distribution over the range  $R_e < R < 5R_e$ . As we average over larger radii, the lenses become increasingly elliptical both in their dark matter and

stars, but dark matter halos are never more elliptical than  $s_{dm} = 1.15$ , while their stars can extend to  $s_* > 1.4$ .

- Three systems have very high stellar ellipticity ( $s_* > 1.6$ ) and correspondingly high alignment between light and dark. One of these – B1608 – is a known merging pair; we suggest that the other two (B0712 and B2016) may also be recent post-merger systems.

- Galaxies with high dark matter ellipticity and weak external shear show very strong alignment between light and dark; those with strong shear ( $\gamma \gtrsim 0.1$ ) can be very highly misaligned. This is reassuring since isolated misaligned galaxies are expected to be unstable.

Our results provide a new constraint on galaxy formation models that must explain the origin of very round dark matter halos (not expected in pure dark matter only simulations), and highly misaligned systems. Such misalignments also present a new challenge for alternative gravity theories in which the light and dark must necessarily be highly correlated.

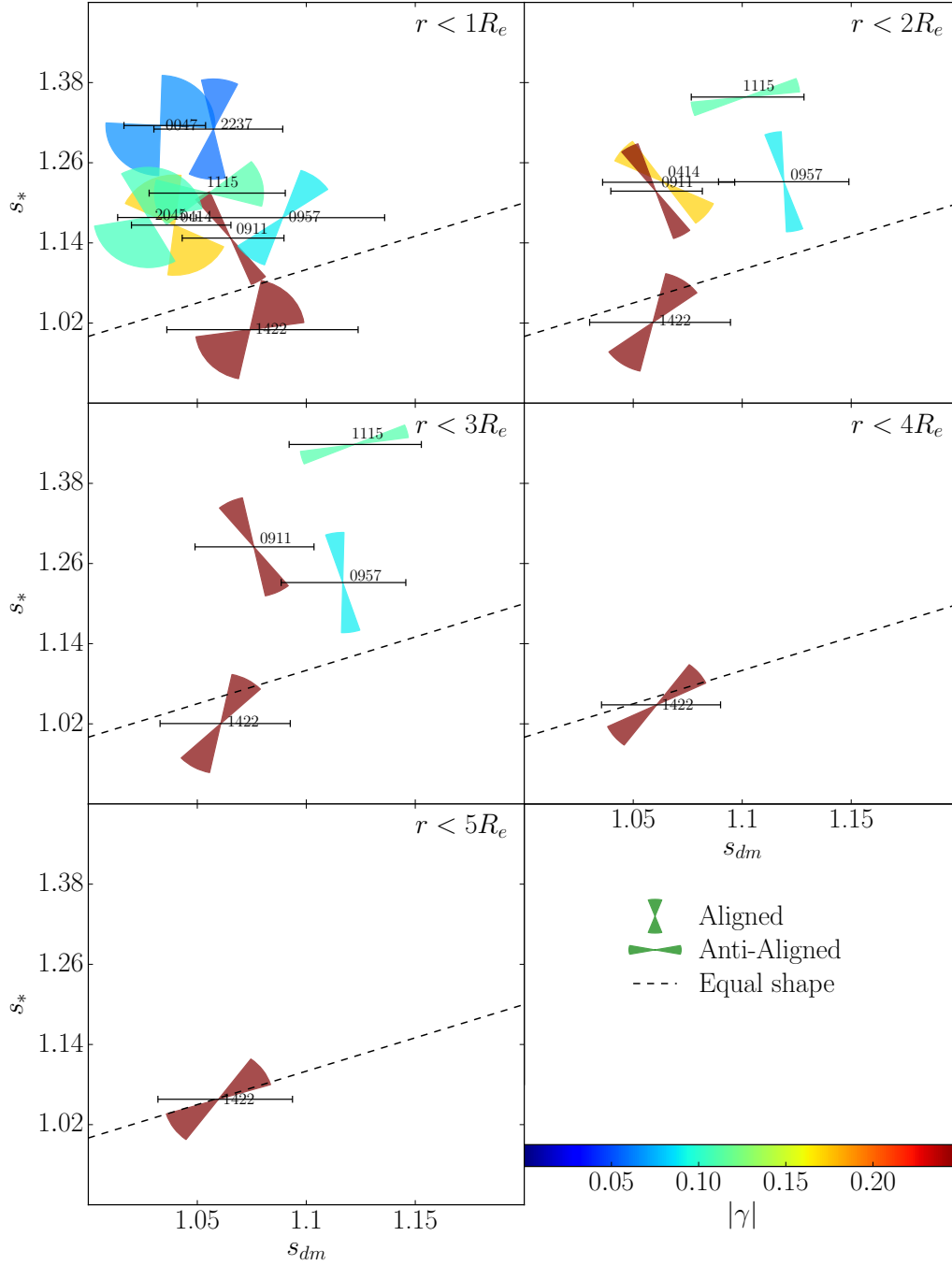


Figure 2.

## 6 ACKNOWLEDGEMENTS

We would like to thank Dominik Leier for useful discussions. JIR would like to acknowledge support from SNF grant PP00P2.128540/1.

## REFERENCES

Auger M. W., Fassnacht C. D., Abrahamse A. L., Lubin

L. M., Squires G. K., 2007, *AJ*, 134, 668  
 Auger M. W., Treu T., Bolton A. S., Gavazzi R., Koopmans L. V. E., Marshall P. J., Moustakas L. A., Burles S., 2010, *ApJ*, 724, 511  
 Blandford R., Narayan R., 1986, *ApJ*, 310, 568  
 Brainerd T. G., Wright C. O., 2000, *ArXiv Astrophysics e-prints*  
 Coles J. P., Read J. I., Saha P., 2014, *ArXiv e-prints*  
 Debattista V. P., Moore B., Quinn T., Kazantzidis S., Maas

R., Mayer L., Read J., Stadel J., 2008, *ApJ*, 681, 1076  
 Debattista V. P., Roškar R., Valluri M., Quinn T., Moore B., Wadsley J., 2013, *MNRAS*, 434, 2971  
 Dubinski J., 1994, *ApJ*, 431, 617  
 Dubinski J., Carlberg R. G., 1991, *ApJ*, 378, 496  
 Ferreras I., Mavromatos N. E., Sakellariadou M., Yusaf M. F., 2012, *Phys. Rev. D*, 86, 083507  
 Ferreras I., Saha P., Burles S., 2008, *MNRAS*, 383, 857  
 Ferreras I., Saha P., Williams L. L. R., 2005, *ApJ*, 623, L5  
 Helmi A., 2004, *ApJ*, 610, L97  
 Hoekstra H., Yee H. K. C., Gladders M. D., 2004, *ApJ*, 606, 67  
 Ibata R., Lewis G. F., Irwin M., Totten E., Quinn T., 2001, *ApJ*, 551, 294  
 Jing Y. P., Suto Y., 2002, *ApJ*, 574, 538  
 Katz N., Gunn J. E., 1991, *ApJ*, 377, 365  
 Kazantzidis S., Kravtsov A. V., Zentner A. R., Allgood B., Nagai D., Moore B., 2004, *ApJ*, 611, L73  
 Keeton C. R., Kochanek C. S., Falco E. E., 1998, *ApJ*, 509, 561  
 Kochanek C. S. et al., 2000, *ApJ*, 543, 131  
 Koopmans L. V. E., Treu T., Bolton A. S., Burles S., Moustakas L. A., 2006, *ApJ*, 649, 599  
 Leier D., Ferreras I., Saha P., 2012, *MNRAS*, 424, 104  
 Lux H., Read J. I., Lake G., Johnston K. V., 2012, *MNRAS*, 424, L16  
 Macciò A. V., Dutton A. A., van den Bosch F. C., Moore B., Potter D., Stadel J., 2007, *MNRAS*, 378, 55  
 Mandelbaum R., Hirata C. M., Broderick T., Seljak U., Brinkmann J., 2006, *MNRAS*, 370, 1008  
 Mortlock D. J., Turner E. L., 2001, *MNRAS*, 327, 552  
 Natarajan P., Refregier A., 2000, *ApJ*, 538, L113  
 Navarro J. F., Frenk C. S., White S. D. M., 1996, *ApJ*, 462, 563  
 Parker L. C., Hoekstra H., Hudson M. J., van Waerbeke L., Mellier Y., 2007, *ApJ*, 669, 21  
 Read J. I., 2014, *Journal of Physics G Nuclear Physics*, 41, 063101  
 Read J. I., Moore B., 2005, *MNRAS*, 361, 971  
 Schneider P., Ehlers J., Falco E. E., 1992, *Gravitational Lenses*  
 Sluse D., Chantry V., Magain P., Courbin F., Meylan G., 2012, *A&A*, 538, A99  
 Treu T., Gavazzi R., Gorecki A., Marshall P. J., Koopmans L. V. E., Bolton A. S., Moustakas L. A., Burles S., 2009, *ApJ*, 690, 670  
 Treu T., Koopmans L. V., Bolton A. S., Burles S., Moustakas L. A., 2006, *ApJ*, 640, 662  
 van Uitert E., Hoekstra H., Schrabback T., Gilbank D. G., Gladders M. D., Yee H. K. C., 2012, *A&A*, 545, A71  
 Warren M. S., Quinn P. J., Salmon J. K., Zurek W. H., 1992, *ApJ*, 399, 405

the dotted lines the 68% confidence interval of these for the dark matter map. Figure 1 is constructed from the ratio of largest to smallest eigenvalue in each case (to measure the shape parameter  $s$ ), and the angle between the dark matter and stellar major axes. Note that the angular scale is always the same for the dark matter and stellar maps, but varies between the different lenses as marked on the Figure axes.

## APPENDIX A: RECONSTRUCTED LENSES

In this appendix, we show the results of our lens modelling for each individual lens (Figures A1, A2, and A3). The panels show, from left to right: the arrival time surface; the surface mass density of the dark matter; and the surface mass density of the stars. The solid lines mark the eigenvalues and eigenvectors of the 2D moment of inertia tensor in each case;

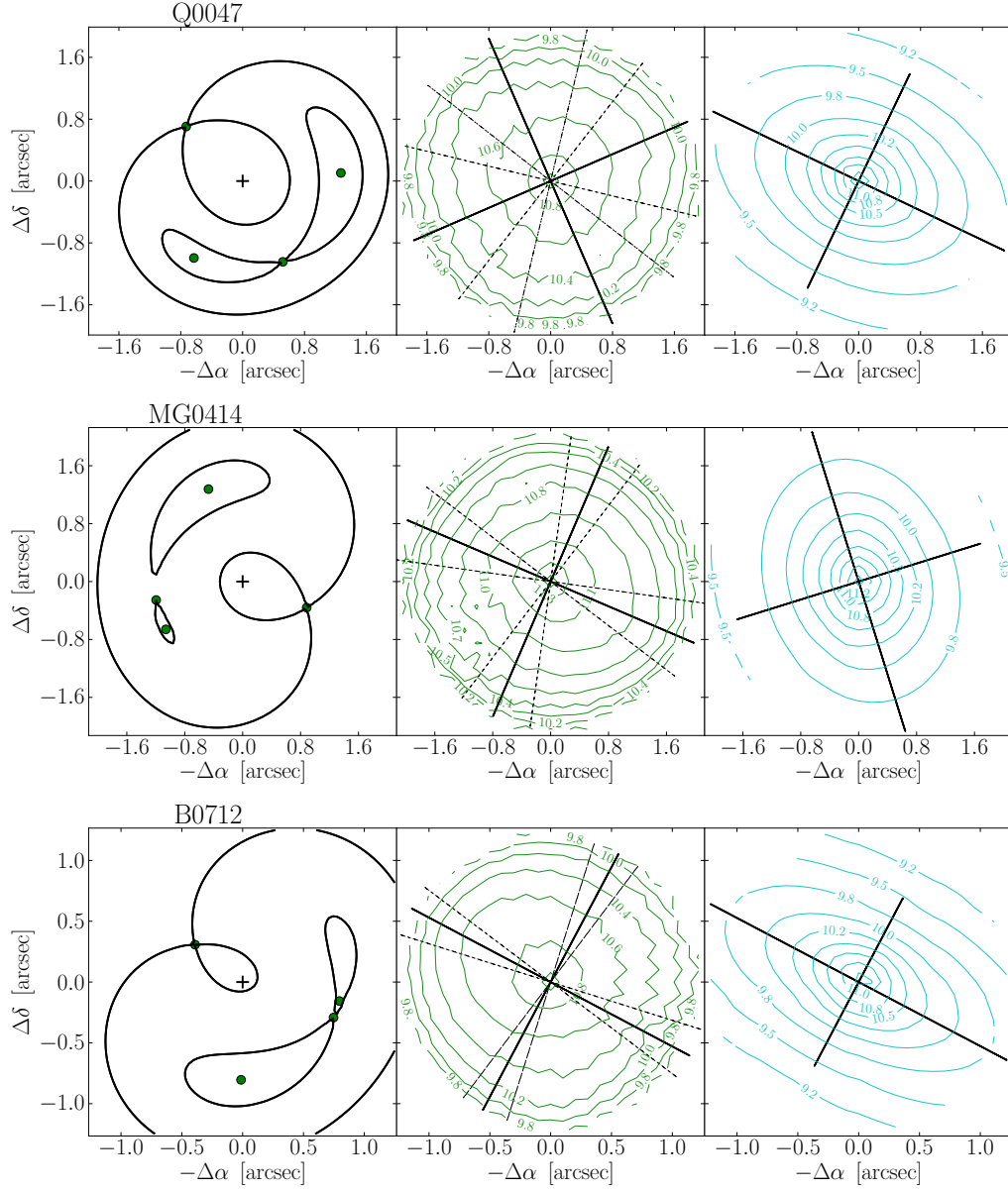


**Figure A1.** The results of our lens modelling for each individual lens. The panels show, from left to right: the arrival time surface (the images are marked by the green circles); the surface mass density of the dark matter; and the surface mass density of the stars. The solid lines mark the eigenvalues and eigenvectors of the 2D moment of inertia tensor in each case; the dotted lines the 68% confidence interval of these for the dark matter map.

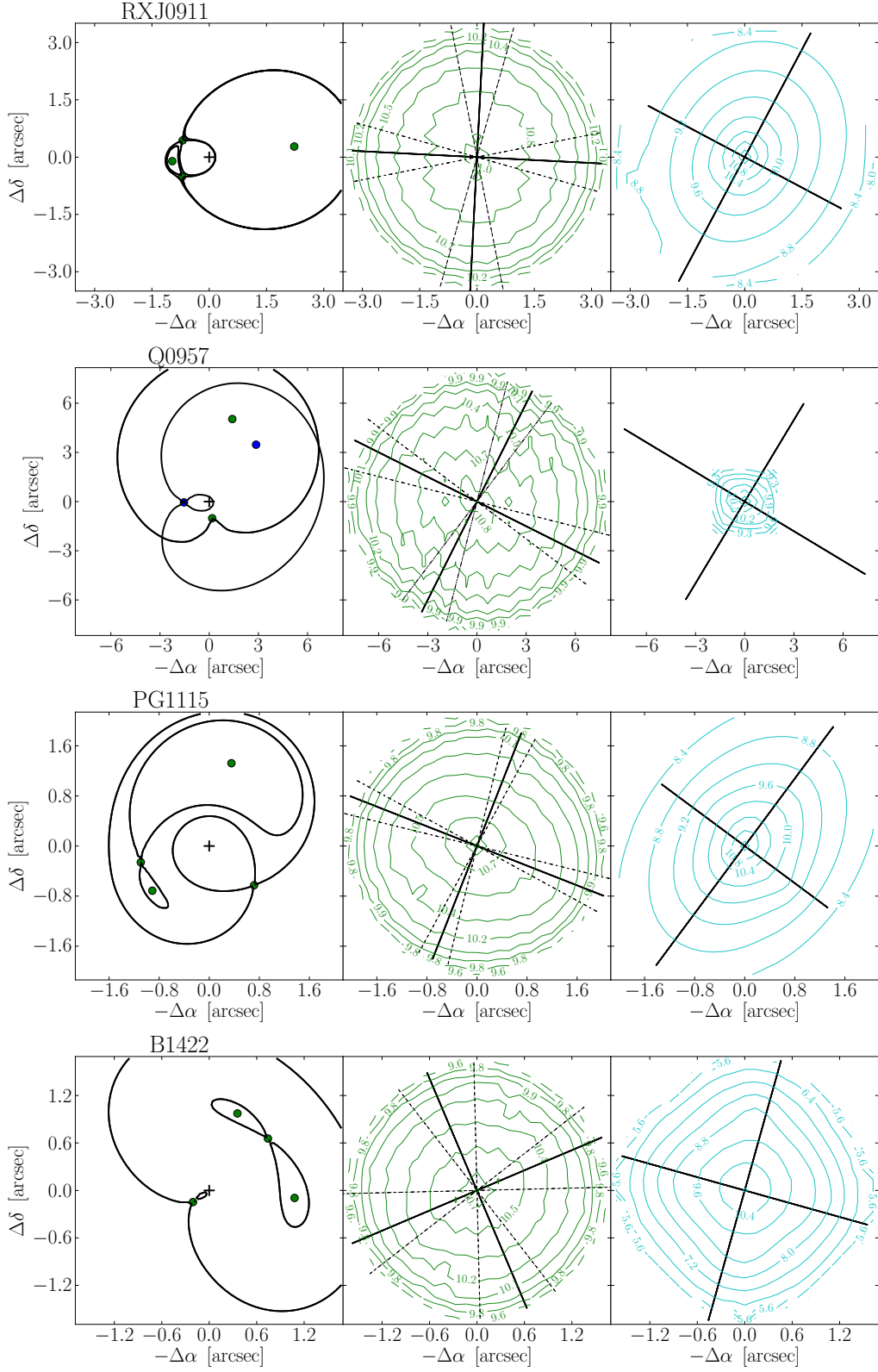


**Figure A2.** The results of our lens modelling for each individual lens. Lines and symbols are as in Figure ??.



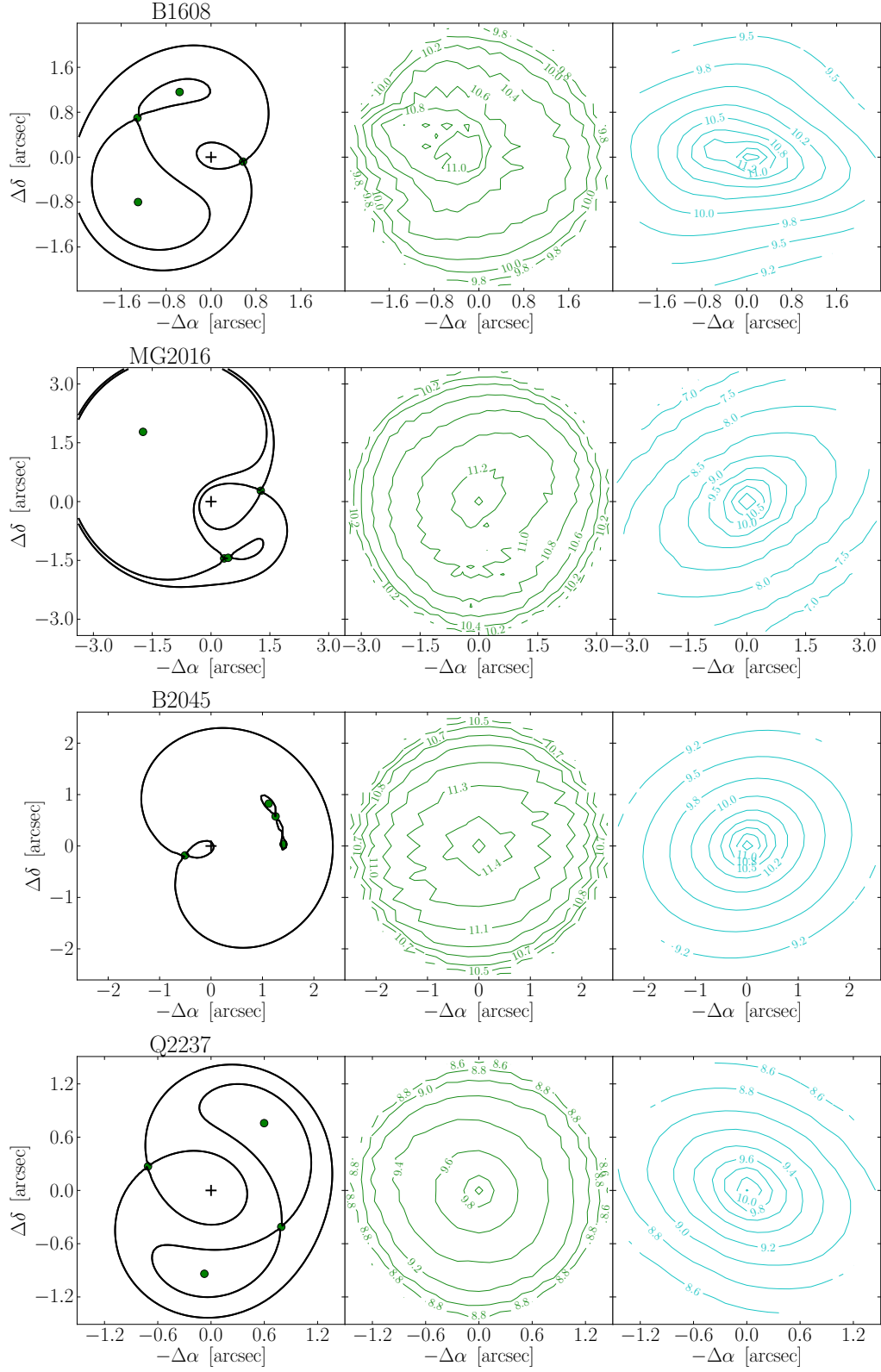


**Figure A3.** The results of our lens modelling for each individual lens. Lines and symbols are as in Figure ??.